

# On Hydraulic and Energetic Efficiencies of Turbine-Type Impeller within Agitation Vessels in Turbulent Flow Regime

Masanori Yoshida\*, Hiromu Ebina, Hayato Shirosaki, Kohei Ishioka, and Koki Oiso

Department of Applied Sciences, Muroran Institute of Technology, 27-1, Mizumotocho, Muroran 050-8585, Japan

\*Corresponding author: Masanori Yoshida, Department of Applied Sciences, Muroran Institute of Technology, 27-1, Mizumotocho, Muroran 050-8585, Japan, Phone: +81-143-46-5761, E-mail: myoshida@mmm.muroran-it.ac.jp

Received Date: November 10, 2014 Accepted Date: December 12, 2014 Published Date: December 18, 2014

Citation: Masanori Yoshida, et al. (2014) On Hydraulic and Energetic Efficiencies of Turbine-Type Impeller within Agitation Vessels in Turbulent Flow Regime. J Chem Proc Eng 1: 1-5.

## Abstract

This study provides an indication of a turbine-type impeller as an agitator within the baffled and unbaffled vessels when the liquid viscosity is varied in the turbulent flow regime. Measurement of the velocity of the liquid flow was performed in the impeller swept region of vessels, namely, the flow path between the neighboring blades of the rotating impeller, abreast of that of the torque of the shaft attached with the impeller. Hydraulic and energetic efficiencies of the impeller were determined on the basis of the experimental data on the internal flow and power of the impeller. It followed with the unbaffled vessel that the efficiencies made a conflicting assessment for the effect of viscosity. As the viscosity was increased, a tendency for the hydraulic efficiency to increase and that for the energetic one to decrease were observed, the efficiencies being demonstrated to reflect elementally the power characteristics of the impeller.

**Keywords:** Agitation vessel; Turbine-type impeller; Efficiency; Turbulent flow

## Introduction

Vessel type apparatuses that are agitated by mechanically rotating impellers are commonly used in industrial applications of chemical processes. Dynamics of the bulk flow produced by an impeller is primarily addressed because the impeller is essential in the apparatus. The ability of the impeller to convert the power input to the liquid flow is referred to as its efficiencies. The higher this quantity is the more effective agitation actions are within the vessel. In the turbulent flow regime as low-viscosity liquids are treated, the baffled vessels are often employed having a disk turbine impeller with six flat blades. For such a configuration of the apparatus, information and knowledge related to the liquid flow within the vessel have been accumulated for utilization in operational and geometrical design[1]. For the turbine type impeller, however, we have insufficiently indications in terms of the efficiencies when the condition on the baffle of vessel and that on the viscosity of liquid were varied.

An aim of this study is to determine the efficiencies of the turbine type impeller with variation of the liquid viscosity for the vessels with and without the baffles, respectively. The

efficiencies were calculated through measurements of the impeller shaft torque and liquid flow velocity. With the help of the efficiencies, the power characteristics were compared between the baffle and viscosity conditions.

## Impeller Efficiencies

To the rotating impeller as an agitator, the power is inputted through the drive shaft. The impeller transmits partially the power to the liquid of the impeller inflow on its blades, with viscous losses in the impeller swept region. The power outputted from the impeller is converted to the impeller outflow. The power other than the portion corresponding to the kinetic energy in the impeller inflow is dissipated entirely within the vessel except for the impeller swept region as in the impeller discharge stream, the primary circulation loops and the wall region along the vessel and adjacent baffles[2]. Efficiencies of the impeller in the two phases for the phenomena in the impeller swept region and that in the rest have been defined to compare the power characteristics.

One for the former phase of the energy cascade is a hydraulic efficiency[3] and it is defined as follows:

$$E_h = P_{out} / P_{in} = N_{pout} / N_{pin} \quad (1)$$

where  $P_{in}$  is the power that the drive shaft inputs to the im-

PELLER, namely, the power consumption of the impeller, and  $P_{out}$  is the power that the impeller outputs to the liquid through its blades. Here,  $P_{out}$  is defined as the power that does not contain the portion converted to turbulences of the impeller outflow. Additionally,  $N_p$ s are the impeller power numbers where the respective powers are expressed in a dimensionless form. The former power is evaluated by measuring the torque of the drive shaft,  $T_s$ , under the determined impeller rotation rate,  $N_r$ , from the following equation:

$$P_{in} = 2\pi N_r T_s \quad (2)$$

The latter one is estimated by analysis of the internal liquid flow of the impeller where the angular momentum theory is applied. Let be the control surfaces and volume in the impeller swept region as depicted in Figure 1. For the flow, we consider the assumptions as

- (1) Liquid flows in the control volume across surfaces 1 and 3 and flows out across surface 2.
- (2) Liquid flows circumferentially and radially through the path between the neighboring blades of the rotating impeller.
- (3) The viscous force on the blade surfaces and the forces on the control surfaces are beyond consideration.
- (4) The angular momentum of liquid inflowing at any radial position is equal to that of a liquid at the related position within the rotating impeller.

The moment on the shaft attached with the impeller is given as the time rate of change of the angular momentum. Expressing the power in relation to the circumferential and radial velocities,  $v_\theta$  and  $v_r$ , of the internal flow,

$$P_{out} = \Sigma \{ [(\rho v_r S)_{i+1} + (\rho v_r S)_i] / 2 \} \{ (u v_\theta)_{i+1} - (u v_\theta)_i \} \quad (3)$$

In Eq. (3),  $S$  is the area of the surface normal to the radial direction,  $u$  is the velocity of impeller rotation that changes depending on the radial position.  $\rho$  is the liquid density, and it was treated as constant. Calculation of  $P_{out}$  from the equation is made using  $v_{r,s}$  and  $v_{\theta,s}$  through the flow measurement. Then,  $E_h$  is experimentally determined with  $P_{in}$  and  $P_{out}$ .

For the latter phase of the energy cascade, another energetic efficiency has been occasionally employed[4-6]. This is represented by the parameters such as the impeller power number,  $N_{pin}$ , and liquid flow number due to impeller pumping,  $N_d$  as follows:

$$E_e = N_d^3 / N_{pin} = [Q_d / (N_r D_i^3)]^3 / [P_{in} / (\rho N_r^3 D_i^5)] \quad (4)$$

where  $Q_d$  is the volumetric flow rate of discharged liquid. Equation (4) defines the efficiency as the kinetic energy of liquid discharged through the impeller per unit time, relative to the power input. According to this definition,  $E_e$  does not consider the kinetic energy due to the circumferential flow. When  $P_{in}$  and  $Q_d$  are evaluated based on the torque and flow measurements as mentioned above, the experimental  $E_e$  is determined.

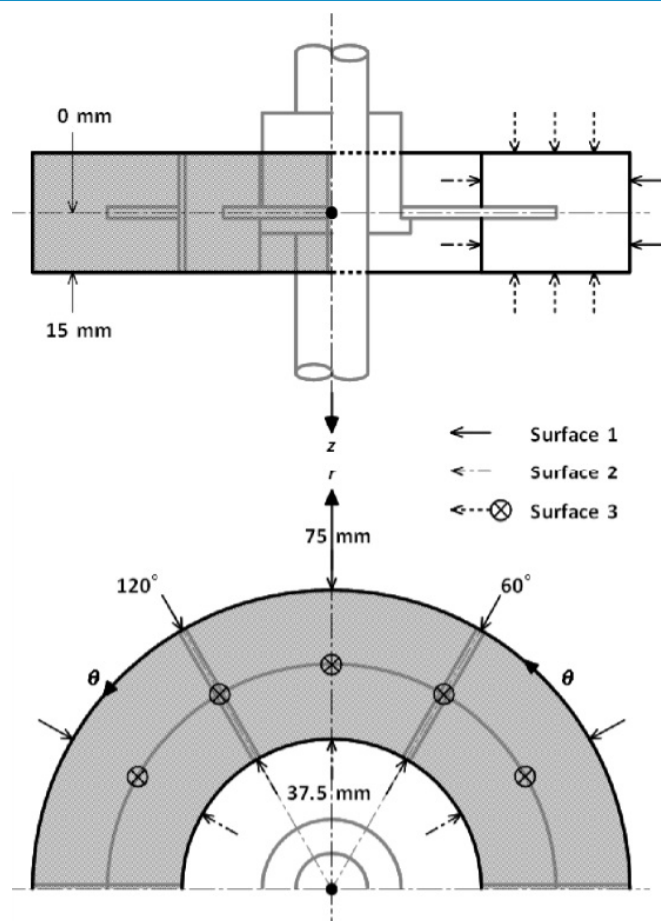


**Figure 1:** Control surfaces and volume in impeller swept region depicted in coordinate system

## Experimental

A schematic diagram of the experimental setup is shown in Figure 2. A fully baffled cylindrical vessel and an unbaffled one with a flat base made of transparent acrylic resin (300 mm in inner diameter,  $D_i$ ) were used. The liquid depth was maintained at  $D_i$ ; 300 mm. A disk turbine impeller with six flat blades (150 mm in diameter,  $D_i$ ) of standard design was used. It had blade width of  $D_i/4$  and height of  $D_i/5$ . The impeller was set at a height of  $0.5D_i$  from the vessel bottom. The impeller rotation rate was set to 100 rpm. The impeller power consumption was determined by measuring the torque with strain gauges fitted onto the shaft[7].

Tomographic visualization of the internal liquid flow of the impeller was done on the different horizontal planes in the impeller swept region of vessels, using the particle suspension method. Additionally, the flow velocity was measured using two-dimensional particle tracking velocimetry (PTV). The axial flow was out of examination. Polystyrene particles (approximately 0.05 mm in diameter and 1.03 g/cm<sup>3</sup> in density) were used as tracers. The liquid phase was water or 50 wt% glycerol aqueous solution. With the respective liquids, the impeller Reynolds numbers were 41900 and 8360, indicating that the bulk liquid flow was turbulent. Images were recorded using a video camera. A 0.5 W laser light sheet adjusted to 2 mm thickness was used for lighting. Lighting was collimated to illuminate the different horizontal planes covering the lower half of the impeller blade. Its height, measured as the distance

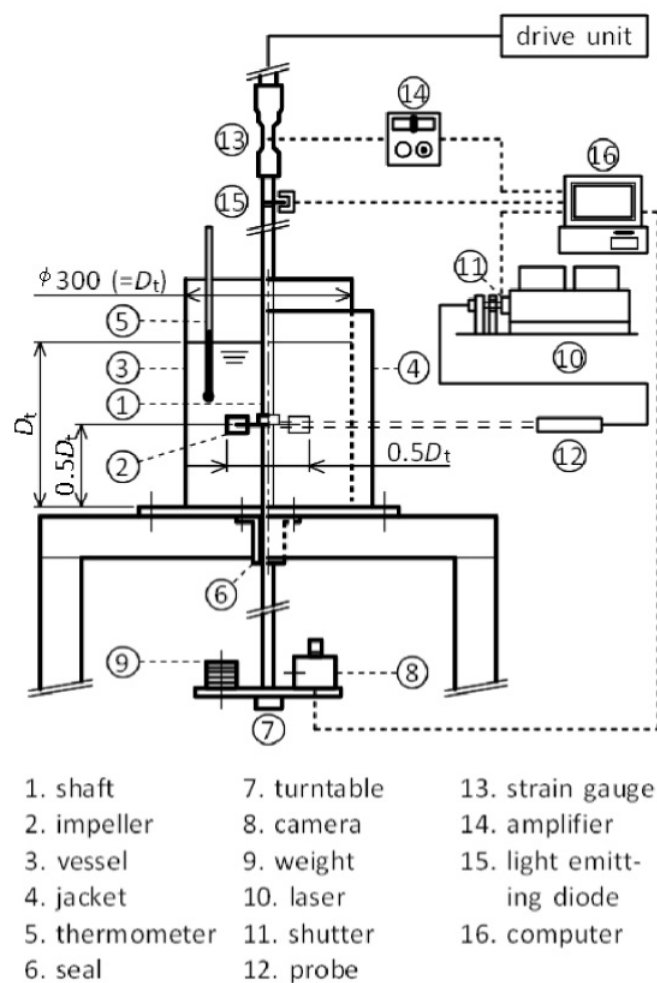


**Figure 2:** Schematic diagram of experimental apparatus (dimensions in mm)

between the centerline of the impeller blade and that of the light sheet, was varied: 1-17 mm. No examination was run for the upper half of the blade. In subsequent analyses, calculations were made on the assumption of vertical symmetry. The circumferential and radial velocities of liquid flow were examined based on pictures taken with the camera set on a turntable underneath the vessel. The table was attached on the same shaft as that driving the impeller. Details of settings for analysis in PTV incorporating the binary cross-correlation method[8] were described in a previous paper[9]. The coordinate system defined on the horizontal and vertical planes is presented in Figure 1. Cylindrical coordinates were used: The origin was designated as the intersection between the shaft centerline and the plane including the impeller blade centerline. The circumferential angle was measured in the orientation depicted in Figure 1. After setting the two instantaneous images in series, the liquid flow velocity through a section ( $2.5 \times 2.5 \text{ mm} = 12.5 \times 12.5 \text{ pixels}$ ) in the test area was determined as the vector based on the difference in position between the tracer particles identified on the composite image and the time between camera frames (1/1000 s). Velocity vectors collected during 40 rotations of the impeller were averaged, being weighted for the distance between the measured point and the section center.

## Results and Discussion

Examination of the internal flow of the impeller proved that its velocity was differed at the axial, circumferential and radial positions. The complicated profile of the flow velocity was coordinated in terms of the circumferential and radial components averaged for the circumferential and axial directions. Figure 3 shows changes of the average velocities,  $v_\theta$  and  $v_r$ , with the radial distance,  $R$ , when the liquid viscosity was varied for each vessel with and without the baffles. Independent of the baffle and viscosity conditions,  $v_\theta$  increased along the flow path between the blades as  $R$  increased and leveled off near the path exit ( $R=75 \text{ mm}$ ). On the other hand,  $v_r$  increased over the entire  $R$  range. For the difference depending on the baffle condition, it was found that  $v_\theta$  was larger without the baffles, but  $v_r$  exhibited the opposite tendency. With increase of the viscosity, the velocities tended to have smaller values in most positions under the respective baffle conditions.

On the basis of the experimental data including those on the power measurement, the impeller power number due to the power input,  $N_{pin}$ , and the liquid discharge flow number,  $N_d$ , were first calculated. The results are summarized in Table 1. These values with the baffles were compared with those reported in the literatures[4,5,10,11] because most of previous reports have been made for the baffled vessels. Accordance was satisfactory and thereby the measurements was confirmed to be used validly for the following analysis.

Then, the hydraulic and energetic efficiencies,  $E_h$  and  $E_e$ , were calculated with the impeller power number due to the power output,  $N_{pout}$ . The results are added to Table 1. Under the both viscosity conditions,  $E_h$  values without the baffles were larger than those with the baffles. This difference is explained to indicate the difference of viscous losses in the internal flow of the impeller. As the viscosity was increased, decreased and increased tendencies of  $E_h$  were found for the baffled and un-

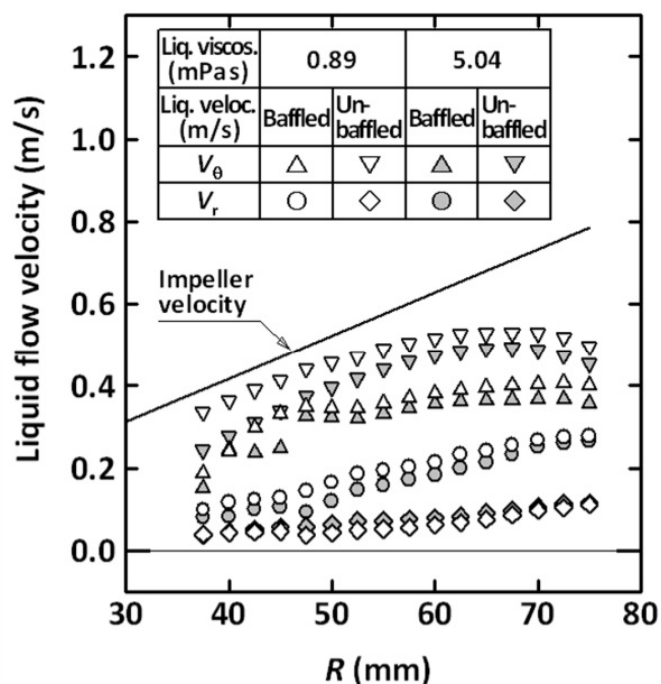


**Figure 3:** Changes of average flow velocities as viewed from radial position



**Table 1:** Impeller efficiencies calculated based on measurements on internal flow and power

Liquid viscosity (mPa s)	Baffle	$N_{pin}$ (-)	$N_{pout}$ (-)	$N_d$ (-)	$E_h$ (-)	$E_e$ (-)
0.89	with	5.0	1.33	0.697	0.266	0.0679
	without	1.2	0.415	0.280	0.346	0.0184
5.04	with	5.0	0.954	0.670	0.191	0.0603
	without	1.4	0.514	0.290	0.367	0.0174

baffled vessels, respectively. This suggests that the power transmission of the impeller is affected by the viscosity of liquid as well as the baffles of vessel [12, 13], although the impeller was operated in the turbulent flow regime. As mentioned above, the internal flow of the impeller has non-uniform velocity profiles. Such a flow field formed depending on the liquid viscosity could make the different level of viscous losses, resulting in the different  $E_h$  values. Table 1 includes  $E_e$  values and those were larger with the baffles for the both liquids of the viscosities. The effect of viscosity for  $E_e$  to decrease was in common to the baffled and unbaffled vessels. According to  $E_e$ , the bulk liquid flow is predicted to be reduced with increase of the viscosity, being improved by the baffles. These results are considered to reflect the dependence of local flows, so-called near-wall flows, on the liquid viscosity because the liquid flow within the vessel can be more or less affected by the solid wall.

Comparison of the effect of viscosity in terms of the two efficiencies,  $E_h$  and  $E_e$ , made a conflicting assessment for the unbaffled vessel. That is, larger  $E_h$  and  $E_e$  were shown with increased and decreased viscosities, respectively. Such an increased  $E_h$  in the unbaffled vessel would be attributable to a weakened forced vortex flow [14] as supported by the result (in Table 1) that the discharge flow number,  $N_d$ , increased slightly with increase of the viscosity [15]. An enhanced discharge flow can cause an increase of the viscous losses in the liquid flow within the vessel and then might produce the decreased  $E_e$ . Combined use of the two efficiencies is demonstrated to be useful for energy consideration of the liquid flow within the vessel. It enables elemental assessment of the impeller power characteristics.

## Conclusions

Power characteristics of the turbine-type impeller were considered in terms of the hydraulic and energetic efficiencies when the baffle condition for vessel and the viscosity condition for liquid were varied. For the unbaffled vessel, the efficiencies gave the different indications of the effect of viscosity. Combined use of the efficiencies was recommended for elemental assessment of the impeller power characteristics.

## Nomenclature

$D_i$	impeller diameter, mm
$D_t$	vessel diameter, mm
$E_e$	energetic impeller efficiency
$E_h$	hydraulic impeller efficiency
$N_d$	liquid discharge flow number
$N_{pin}$	impeller power number due to $P_{in}$
$N_{pout}$	impeller power number due to $P_{out}$

$N_r$	impeller rotation rate, rpm
$P_{in}$	impeller power input, W
$P_{out}$	impeller power output, W
$Q_d$	volumetric flow rate of discharged liquid, m <sup>3</sup> /s
$R$	radial distance, mm
$S$	area of surface normal to radial direction, m <sup>2</sup>
$T_s$	impeller shaft torque, Nm
$u$	velocity of impeller rotation, m/s
$v_r$	radial velocity component of liquid flow, m/s
$v_\theta$	circumferential velocity component of liquid flow, m/s
$Z$	axial distance, mm
$\Theta$	circumferential angle, deg
$\rho$	density of liquid, g/cm <sup>3</sup>

## References

- 1) Lee KC, Yianneskis M (1998) Turbulence properties of the impeller stream of a Rushton turbine. *AIChE J* 44: 13-24.
- 2) Bruha O, Bruha T, Fort I, Jahoda M (2007) Dynamics of the flow pattern in a baffled mixing vessel with an axial impeller. *Acta Polytechnica* 47: 17-26.
- 3) Fort I (2011) On hydraulic efficiency of pitched blade impellers. *Chem Eng Res Des* 89: 611-615.
- 4) Nienow AW (1997) On impeller circulation and mixing effectiveness in the turbulent flow regime. *Chem Eng Sci* 52: 2557-2565.
- 5) Fentiman NJ, St Hill N, Lee KC, Paul GR, Yianneskis M (1998) A novel profiled blade impeller for homogenization of miscible liquids in stirred vessels. *Chem Eng Res Des* 76: 835-842.
- 6) Wu J, Graham LJ, Nguyen B, Mehidi MNN (2006) Energy efficiency study on axial flow impellers. *Chem Eng Process* 45: 625-632.
- 7) Yoshida M, Ito A, Yamagiwa K, Ohkawa A, Abe M, et al. (2001) Power characteristics of unsteadily forward-reverse rotating impellers in an unbaffled aerated agitated vessel. *J Chem Technol Biotechnol* 76: 383-392.
- 8) Uemura T, Yamamoto F, Sachikawa M (1990) High-speed image analysis algorithm for particle tracking velocimetry. *Trans Visualization Soc Japan* 10: 196-202.
- 9) Yoshida M, Shigeyama M, Hiura T, Yamagiwa K, Ohkawa A, et al. (2007) Liquid flow in impeller region of an unbaffled agitated vessel with unsteadily forward-reverse rotating impeller. *Chem Eng Comm* 194: 1229-1240.
- 10) Mishra VP, Joshi JB (1993) Flow generated by a disc turbine: Effect of impeller diameter, impeller location and comparison with other radial flow turbines. *Chem Eng Res Des* 71: 563-573.
- 11) Pinho FT, Piqueiro FM, Proenca MF, Santos AM (1997) Power and mean flow characteristics in mixing vessels agitated by hyperbolic stirrers. *Can J Chem Eng* 75: 832-842.
- 12) Gray JB (1966) Flow patterns, fluid velocities, and mixing in agitated vessels. In: Uhl VW, Gray JB, editors. *Mixing, Theory and Practice* 1. Academic Press. P 179-278.
- 13) Mavros P, Xuereb C and Bertrand J (1998) Determination of 3-D flow fields in agitated vessels by laser Doppler velocimetry: Use and interpretation of RMS velocities. *Chem Eng Res Des* 76: 223-233.
- 14) Rousseaux JM, Muhr H, Plasari E (2001) Mixing and micromixing times in the forced vortex region of unbaffled mixing devices. *Can J Chem Eng* 79: 697-707.
- 15) Glover GMC, Fitzpatrick JJ (2007) Modelling vortex formation in an unbaffled stirred tank reactors. *Chem Eng Sci* 127: 11-22.

**Submit your manuscript to a JScholar journal and benefit from:**

- ¶ Convenient online submission
- ¶ Rigorous peer review
- ¶ Immediate publication on acceptance
- ¶ Open access: articles freely available online
- ¶ High visibility within the field
- ¶ Better discount for your subsequent articles

Submit your manuscript at  
<http://www.jscholaronline.org/submit-manuscript.php>